PROCEEDINGS, Thirty-Seventh Workshop on Geothermal Reservoir Engineering
Stanford University, Stanford, California, January 30 - February 1, 2012
SGP-TR-194

A THERMAL-HYDROLOGICAL-CHEMICAL MODEL FOR THE ENHANCED GEOTHERMAL SYSTEM DEMONSTRATION PROJECT AT NEWBERRY VOLCANO, OREGON

Eric Sonnenthal[1], Nicolas Spycher[1], Owen Callahan[2], Trenton Cladouhos[2], and Susan Petty[2]

[1]Earth Sciences Division, Lawrence Berkeley National Laboratory
Berkeley, CA, 94720 USA
e-mail: elsonnenthal@lbl.gov
[2]AltaRock Energy, Inc.
Seattle, WA, 98103 USA

ABSTRACT

Newberry Volcano in Central Oregon is the site of a Department of Energy funded Enhanced Geothermal System (EGS) Demonstration Project. Stimulation and production of an EGS is a strong perturbation to the physical and chemical environment, giving rise to coupled Thermal-Hydrological-Mechanical-Chemical (THMC) processes leading to permeability changes as a result of mineral dissolution and precipitation, rock deformation, and fracture reactivation. To evaluate these processes, and to help guide EGS stimulation and reservoir development strategies, a combined native-state and reservoir model of the west flank of Newberry Volcano was created that encompasses the planned stimulation zone and a several km region of the west flank from the surface down to the supercritical region, likely close to a postulated cooling intrusive body. Temperature and pressure distributions were first modeled using TOUGHREACT with boundary conditions estimated from nearby drill holes, and compared to measurements made in the over 3 km deep NWG 55-29 drill hole. With estimates of the porosity and heat capacities for the major hydrogeologic units, thermal conductivities were calibrated by matching to the measured temperature profile. To simulate the development of the observed hydrothermal mineralogy, a reaction-transport model (THC) was developed using the pre-alteration mineralogy and shallow groundwater chemistry as the initial geochemical conditions, assuming that modeled temperature and pressure distributions were relatively constant over several thousand years. Close correspondence of modeled and observed epidote distributions support the observation that past hydrothermal activity took place under thermal gradients similar to current values, whereas calcite and sulfide abundances at depth likely require a magmatic gas component. Multicomponent geothermometry was used to estimate potential

temperatures of equilibration of waters, and to evaluate the effects of kinetics on calculated mineral equilibration temperatures. The ultimate goal will be to capture both the local chemical and mechanical changes in the rock owing to stimulation as well as the potential long-term response and sustainability of the larger-scale geothermal reservoir.

INTRODUCTION

Newberry Volcano in central Oregon, USA is the site of a planned Enhanced Geothermal System Demonstration Project, funded by the Department of Energy. The purpose of the coupled THMC model is to capture both the local chemical and mechanical changes in the rock owing to stimulation as well as the potential long-term response and sustainability of the geothermal reservoir. In this paper we describe the development of the THC model, including the numerical model set-up, estimation/calibration of the hydrological and thermal parameters, and the geochemical inputs. As a first step to developing the THMC reservoir model, it is necessary to simulate the current temperature distribution and the development of the observed alteration mineralogy, i.e. the “native-state” model. Simulation of the native-state is essential for testing the validity of the geochemical model, the thermodynamic and kinetic parameters, and the conceptual model for the present hydrothermal system. It also gives important constraints on the fluid flow and reactivity of the fracture system that will be stimulated and must sustain long-term injection and production.

THC NUMERICAL MODEL

Model Boundaries

An elevation map of Newberry Volcano, with many of the deeper drill holes, is shown in Figure 1. The most recent drill hole NWG 55-29 is centered on the west flank of the volcano, near point B, with section C-C' crossing close by.

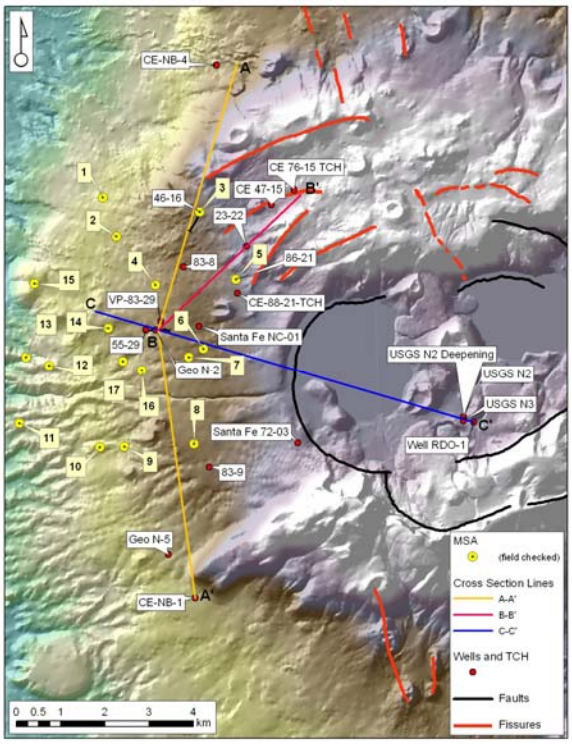

Figure 1: Map of Newberry Volcano, surface-based drill holes, and cross-section locations.

The numerical model boundary was chosen that was large enough to encompass the planned stimulation, injection, and production zones of the EGS reservoir around NWG 55-29. The eastern boundary extends to one of the ring faults outside the caldera rim and the west boundary extends approximately to the edge of the C-C' cross-section (Figure 2). The eastern boundary was not set at the caldera-bounding fault, because the temperatures at the lower part of the domain would exceed 500°C and thus would be well outside the range of the thermodynamic properties of the flow module and the mineral-water-gas equilibrium constant database. As the geologic model is further developed, and production holes locations are chosen, the model boundaries will be extended into three dimensions.

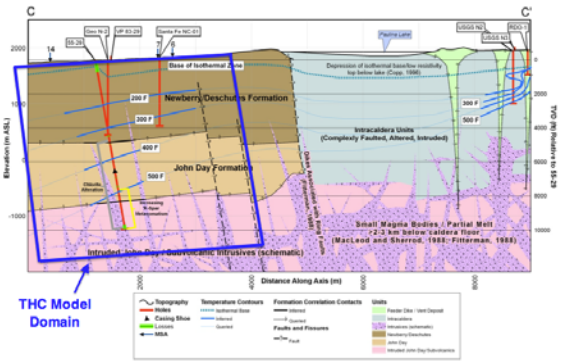

Figure 2: THC model boundaries superimposed on cross-section C-C' (roughly E-NE to W-SW).

The model boundary is also shown superimposed on the cross-section of Sammel et al. (1988), with temperature contours generated by conductive cooling of a rhyolitic magma initially at 850°C (Figure 3). Three hydrologic units were defined on the western flank, denoted as FLOWS 1-3. These layer units do not correspond directly to the units shown in Figure 2. Note that the temperatures in FLOW 3 of Figure 3 are somewhat lower than those in the new cross-section, because of newer measurements from recent deeper drilling on the flank of the volcano. A more complex cross-section depicting potential locations of numerous moderate-sized rhyolitic and basaltic magma chambers is given in Fitterman (1988). However, the overall conceptual model for the hydrothermal system in Sammel et al. (1988) appears to be a good starting point for the THMC model.

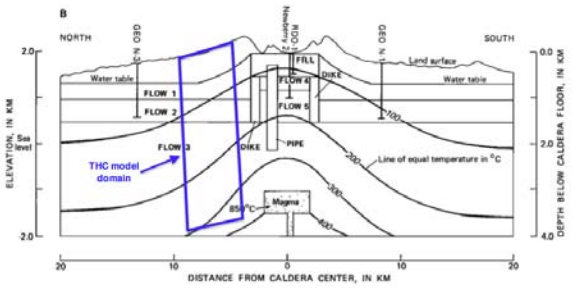

Figure 3: Location (approximate) of the THMC model domain (in blue) superimposed on E-W cross-section from Sammel et al. (1988).

Numerical Mesh

A numerical mesh was developed with the attributes that it could serve as a mesh to evaluate the native state hydrothermal system and also to be used for modeling near-well processes such as injection and stimulation (Figure 4). The gridding was made

progressively finer towards the well, and the two-dimensional mesh is composed of 7070 grid blocks.

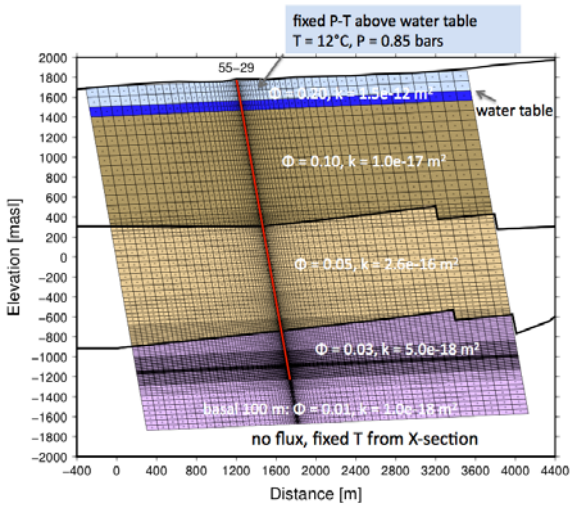

Figure 4: Numerical mesh showing hydrogeologic units, assigned porosity and permeability values, and thermal and hydrological boundary conditions.

A pseudo-three-dimensional mesh for use in flow test simulations was also generated by modification of the volumes of the grid blocks by radial symmetry around the well. The orientation of the well was estimated from the cross-section and has not been updated to reflect the actual trajectory of the well, which is more nearly vertical for the first kilometer, and then progressively changes its angle to about 20 degrees from vertical. Another zone of very fine gridding was placed at the postulated fracture zone (~ -1200 masl) where fluid was lost during the baseline injection test conducted in 2010. Once the locations and orientations of the most important fractures are determined, the gridding will be modified.

Hydrological and Transport Properties

Bulk (fracture + matrix) hydrological properties were for the most part estimated for the major units shown in Figures 2 and 4, with some additions at the top and bottom of the domain (Table 1 and Figure 4).

Table 1. Hydrological Properties

Hydrogeologic Unit	Porosity	Permeability (m^2)
Newberry-Deschutes (upper 300 m)	0.20	1.5×10^{-12}
Newberry-Deschutes	0.10	1.0×10^{-17}
John Day	0.05	2.6×10^{-16}
Intruded John Day	0.03	5.0×10^{-18}
I. John Day (base)	0.01	1.0×10^{-18}

A bulk permeability for the John Day unit of 2.6×10^{-16} m^2 was measured by Spielman and Finger (1998) in the CE 23-22 wellbore (about 3 km NE of NWG 55-29) for the slotted portion of the well over the depth interval from 6488 to 9577 feet. Although the lower 920 feet of the well penetrated "granitic" bedrock, much of the water loss contributing to the bulk permeability was likely at the 6770 foot level. A value of 1.5×10^{-12} m^2 for the near-surface permeability was estimated from groundwater velocity measurements. The Newberry-Deschutes formation permeability (1×10^{-17} m^2) was estimated based on Sammel et al. (1988). Neither field or core-scale permeabilities are available for the site, but porosities were measured on numerous cuttings samples. The values are quite scattered and will need to be reconsidered once a detailed geological model is developed. Although, the current model assumes an effective fracture-matrix permeability, the stimulation models will need to consider multiple continua (e.g., dual permeability).

Simulated Steady-State Pressure and Temperature Distributions

The initial boundary conditions for the modeling are also shown in Figure 4. The base was assumed as a no-flux boundary for flow and fixed temperature. A top zone of 300 meters was assigned a fixed pressure and temperature to approximate the constant temperature region above the water table. The side boundaries were assumed to be no-flux, which causes some issues for the near surface hydrology but is more reasonable for the deep steady-state temperature and pressure distributions. Likely, the model will be extended to the east and west with coarser gridding to allow implementation of a far-field hydrostatic boundary.

For this first phase of the model simulations, without having thermal conductivity measurements on core samples, thermal conductivities for the THC model were calibrated by trial-and-error adjustment to downhole temperature measurements (Table 2). The initial starting value was estimated as 2.00 $Wm^{-1}{}^{\circ}K^{-1}$. The solid (grain) density and the heat capacity are assumed to be the same for all rock units as in Sammel et al. (1988).

Table 2. Calibrated Thermal Properties

Hydrogeologic Unit	Saturated Thermal Conductivity (W/m-°K)
Newberry-Deschutes (upper 300 m)	1.70
Newberry-Deschutes	1.80
John Day	2.15
Intruded John Day	2.20
Intruded John Day (base)	2.20

The fluid temperature and pressure in the current system were modeled assuming a fully water-saturated rock mass. Simulations were performed using TOUGHREACT V2 (Xu et al., 2011). Fractures may be either partially or fully vapor-saturated, but with such low porosities, this assumption does not cause much error in the estimated thermal conductivities. An initial temperature distribution was developed from the contours in Figure 2 and used to make a first estimate of the hydrostatic pressure distribution. Temperatures above 365°C were fixed because TOUGHREACT cannot handle supercritical water. A comparison simulation was also performed using a supercritical version of TOUGH2 (AUTOUGH2; Croucher and O'Sullivan, 2008), which gave temperatures at the drill hole very similar to those of TOUGHREACT. Once the first approximation of the steady-pressure distribution was obtained, the temperature was fixed at the top and bottom boundaries and allowed to reach steady-state concurrently with pressure. A 100,000-year simulation time was found to result in a close approach to steady-state.

Thermal conductivities were modified by trial-and-error so that the temperature profile better matched the measured profile from the October 2008 measurements. Starting from an initial value of 2.0 W/m-°K, it was only necessary to modify the values by about 10% in each direction. The resulting steady-state pressure and temperature distributions and profiles compared to the measured data are shown in Figures 5, 6, and 7.

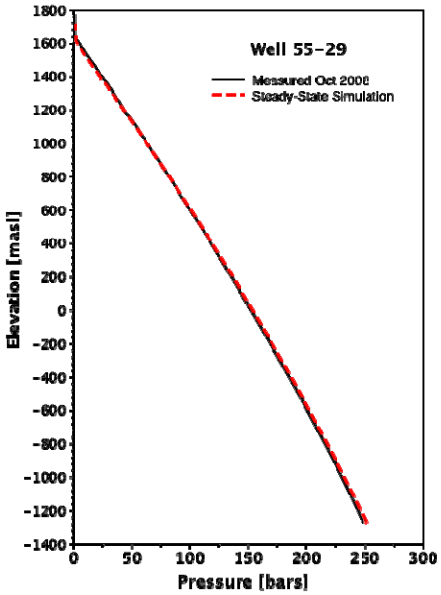

Figure 5: Comparison of simulated and measured pressure profiles from October 2008.

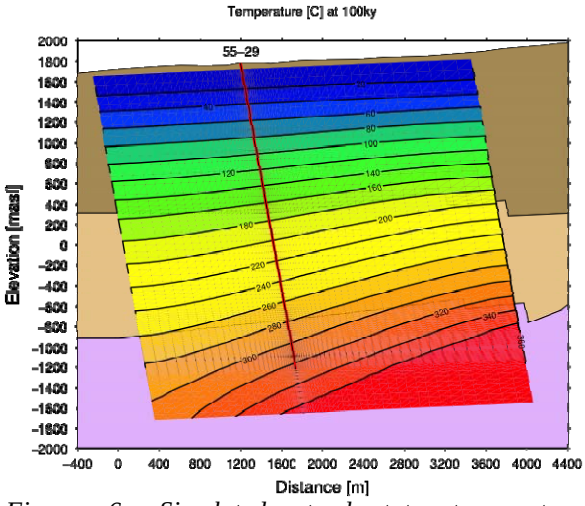

Figure 6: Simulated steady-state temperature distribution, with region of fixed temperature at 365°C.

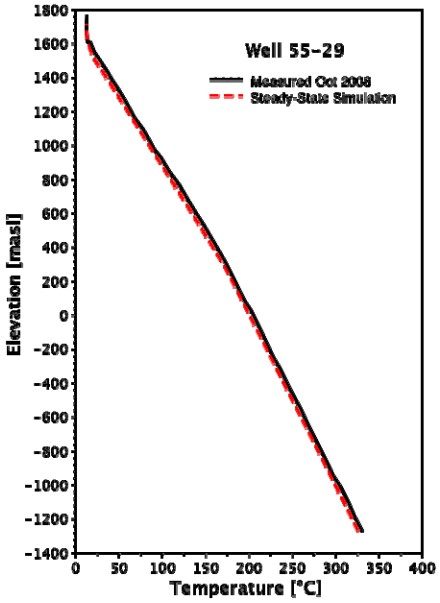

Figure 7: Comparison of simulated and measured temperature profiles from October 2008.

The simulated pressure profile closely matched the hydrostatic distribution in the well. Temperatures were also matched quite closely with modest changes in the thermal conductivities of the units.

Some support for the calibrated thermal conductivities can be given by comparison to measured values on cores from other drill holes. Swanberg et al. (1988) reported thermal conductivity measurements on cores from lavas taken at depths of 1164 to 1219 m in drill hole GEO N-1. Measurements were made on twelve samples from three intervals, giving average values of 1.76, 2.01, and 2.00 $Wm^{-1°}K^{-1}$. These samples are likely correlative to lavas encountered near the lower part

of the Newberry-Deschutes Formation in NWG 55-29. Another series of 9 samples from GEO N-3 at about the same depth range gave an average value of 1.59 $Wm^{-1}K^{-1}$. Because lithologies and porosities vary considerably within these units there is no way to correlate any single set of samples between these drill holes and NWG 55-29, at least 10 km away. Another complicating factor is that measurements were likely performed at room temperature, whereas the calibrations reflect the conductivity at the *in situ* temperature. Acknowledging these uncertainties, though, the calibrated thermal conductivity (1.80 $Wm^{-1}K^{-1}$) of the Newberry-Deschutes unit is within the range observed in the sample measurements.

GEOCHEMICAL MODELING OF GAS AND WATER SAMPLES FROM NWG 55-29

Analyses of noncondensible gases were reported for two gas samples collected directly from the flow line at the sampling separator of NWG 55-29 (Geologica, 2008). Analyses of one water sample collected from the weir box of this well, and one water sample from a nearby water well used for drilling fluids (WW2) were also reported. No condensate was obtained from the gas samples. According to the Geologica report, the water sample from the weir box represents a fluid similar in composition to evaporated local groundwater (likely used for drilling fluid) likely re-equilibrated with calcite and/or other minerals, whereas sampled gases appear to be coming from a geothermal source. In a more recent report (Geologica, 2010) temperatures are estimated from gas geothermometry. The absence of condensate in the gas samples precluded the determination of water to liquid ratios. Because four of the seven applied gas geothermometers required such data, various assumptions were made to constrain gas/liquid proportions at various values, yielding a wide range of temperatures (~117°–321°C), and averaging 258°C. Calculations independent of the gas/water ratio yielded a higher temperature range (~279°–310°C) averaging 293°C.

As part of the current study, an attempt was made to reconstitute the composition of the downhole liquid+gas fluid and derive, from these analyses, possible equilibration temperatures of formation minerals with that fluid. The method is essentially that described previously by Reed and Spycher (1984), whereby gas amounts are stoichiometrically titrated back into liquid samples, and multicomponent speciation calculations with the resulting fluid are carried out over a wide temperature range to assess the saturation indices of minerals likely to have equilibrated with the reconstituted (deep) fluid. The clustering of saturation indices near zero (log(Q/K) = 0, the value at equilibrium) for multiple minerals at any given temperature can then be inferred as a possible temperature of the deep fluid.

These computations require knowledge of the amount of H_2O vapor in the gas phase, as well as the relative proportion of liquid and gas in the discharge (the steam weight fraction). In absence of these data, the steam weight fraction was inferred from the ratio of the Cl concentration reported in the water sample from WW2 (13.8 ppm) to the Cl concentration in the fluid collected in the weir box (646 ppm) (thus assuming conservative behavior of Cl and a negligible potential Cl geothermal or magmatic source), yielding a steam fraction ~ 0.9787 (i.e., equal to 1–13.8/646). It should be noted that groundwater at locations other than WW2 appear to have essentially the same composition as at WW2, but a lower Cl concentration around 3 ppm (e.g., East Lake Hot Spring 5B). The reason for this difference is unclear, and it was decided to also perform computations using the lower Cl concentration, yielding a steam weight fraction ~ 0.9954 (i.e., equal to 1–3/646). The application of these steam weight fractions thus assumes that the difference in Cl concentrations in groundwater and in the fluid from the weir box results from evaporative concentration (boiling) of the groundwater.

Using the steam weight fractions calculated in this manner (and recognizing associated assumptions and their uncertainty), the amount of H_2O vapor in the gas phase was then estimated by varying this parameter until the best clustering of mineral saturation indices near zero was achieved anywhere in the temperature range 150°–350°C. The computations were carried out using a fluid-reconstitution and speciation code in development, designed specifically for geothermometry calculations, and derived from the TOUGHREACT code (Xu et al., 2011). Thermodynamic data were taken from the database compiled by Reed and Palandri (2006).

Computations were first run using the lower steam fraction representing evaporative concentration of water from well WW2. In absence of measured Al data, computations were run assuming Al concentrations fixed by equilibrium with muscovite (Figure 8) or with kaolinite (Figure 9). In the first case (forced equilibration with muscovite), two groups of potential minerals are observed to cluster near the line indicating equilibrium (at log(Q/K) = 0): chlorite-muscovite-paragonite-kaolinite-pyrrhotite-pyrite near 260°C, and epidote-anorthite-muscovite-paragonite-kaolinite-pyrrhotite near 320°C. Note that each group separately (not both together) can be used to infer near-equilibration temperatures of the reconstituted fluid. In the second case (forced

equilibration with kaolinite), one relatively good cluster is observed near 320°C for the group epidote-siderite-anorthite-muscovite-paragonite-kaolinite.

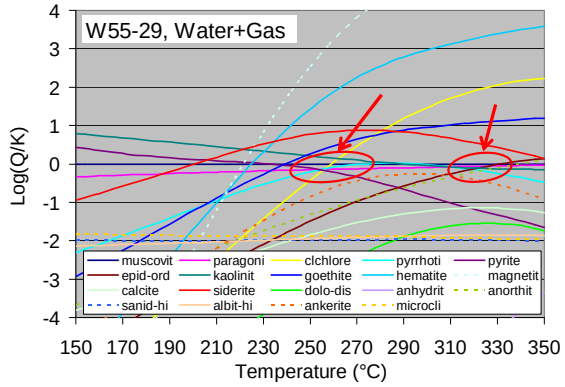

Figure 8: Computed mineral saturation indices (log(Q/K)) as a function of temperature for the reconstituted fluid in NWG 55-29, assuming equilibrium with kaolinite at all temperatures, and assuming a steam weight fraction (0.9787) consistent with evaporative concentration of water from well WW2 (with 13.8 ppm Cl). Arrows indicates clustering areas representing potential near-equilibration temperatures.

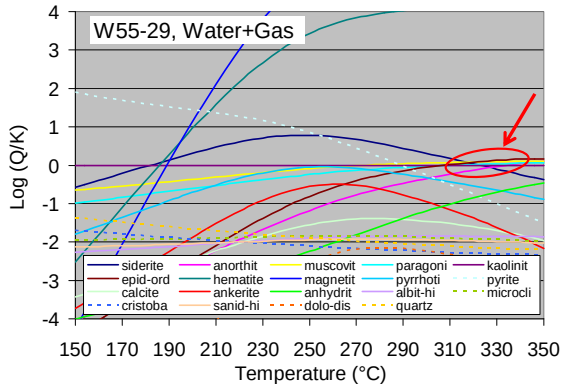

Figure 9: Computed mineral saturation indices (log(Q/K)) as a function of temperature for the reconstituted fluid in NWG 55-29, assuming equilibrium with muscovite at all temperatures, and assuming a steam weight fraction (0.9787) consistent with evaporative concentration of water from well WW2 (with 13.8 ppm Cl). Arrow indicates clustering area representing potential near-equilibration temperatures.

Computations run using the higher steam fraction derived from groundwater Cl concentrations, ~ 3 ppm, yielded a more dilute fluid that remained undersaturated with respect to essentially all potential formation minerals in the temperature range 150°–350°C. This, and the fact that the steam weight fraction in the discharge and amount of H_2O vapor in the wet gas were unknown and had to be estimated, emphasizes the uncertainty of the computation results shown here, and emphasize the need for very careful interpretation. Furthermore, computation results are quite sensitive to the assumed amount of H_2O vapor in the wet gas, and the manual optimization of this value is likely to be non-unique. Nevertheless, it is interesting to note that potential equilibration temperatures inferred by Figures 8 and 9 are consistent with the range of temperatures previously derived from gas geothermometers. If valid, these results would infer some degree of equilibration of fluids from WW2 with some formation minerals (presumably the faster-reacting minerals), but undersaturation with most other formation minerals (presumably the slower-reacting minerals).

NATIVE STATE THC MODEL SIMULATIONS

This section describes THC simulation of the native-state using geochemical data on groundwater described in the previous section and the modeled steady-state pressure and temperature distributions. Simulation of the native-state is essential for testing the validity of the geochemical model, the thermodynamic and kinetic parameters, and the conceptual model for the present hydrothermal system. It also gives important constraints on the fluid flow and reactivity of the fracture system to be stimulated and which must sustain permeability over long-term injection and production.

Primary and Alteration Mineralogy

Mineral assemblages are characterized according to their origin; either those that were present at the time of emplacement/deposition of the lavas, intrusion, pyroclastics, etc., (i.e., primary) or those that formed during subsequent hydrothermal alteration, burial or groundwater interaction. The minerals chosen for the THC model simulations (Table 3) are based primarily on detailed studies of hydrothermal alteration by Keith and Bargar (1988), Bargar and Keith (1999), and recent mud log descriptions from NWG 55-29.

Table 3. List of Primary and Potential Secondary Minerals in the THC Model

Primary Minerals	Potential Secondary Minerals
Albite	Calcite
Anorthite	Siderite
Microcline	Ankerite
Sanidine	Dolomite
Diopside	Anhydrite
Hedenbergite	Chalcedony

Phlogopite	Quartz
Annite	Microcline
Muscovite	Muscovite
Quartz	Paragonite
Cristobalite	Illite
Magnetite	Nontronite-Ca
	Nontronite-Mg
	Nontronite-Na
	Nontronite-K
	Kaolinite
	Epidote
	Daphnite
	Clinochlore
	Heulandite
	Laumontite
	Analcite
	Magnetite
	Hematite
	Goethite
	Pyrite
	Pyrrhotite

Distributions of minerals were not tied to specific flows or intrusives and were just assigned to roughly approximate the average bulk abundances in the units. The units with more basaltic rocks were given larger proportions of pyroxenes, plagioclase, and magnetite, whereas tuffs and rhyolitic rocks were assigned more sanidine and cristobalite with fewer mafic minerals. The "Intruded John Day", having extensive intrusion of granodiorite, was assigned more quartz, microcline, and muscovite with less mafics because of the fewer basaltic rocks in this unit. This will be updated as the model is refined, but for the first set of simulations the goal was just to capture the overall behavior of the system.

In the current mineral description, the solid solution phases are represented as their endmembers (e.g., chlorite is represented as clinochlore and daphnite). This is usually easier numerically than treating minerals as solid solutions, but potentially leads to unrealistic mineral assemblages. As more data is gained from field studies of fracture mineralogy, the list may also change, especially with respect to minor phases that may control certain isotopic systems, or changes induced by stimulation and injection that result in effects unlike that of the natural system.

Thermodynamic and Kinetic Data

Thermodynamic data were derived from the SOLTHERM database (Reed and Palandri, 2006). This database has been specifically developed for the study of hydrothermal alteration and was used for the geothermometry calculations presented previously.

Kinetic data were derived from various sources (e.g., Palandri and Kharaka, 2004) or assumed to be the same as similar minerals. Reactive surface areas were estimated to be in the range of 1-20 cm^2/g mineral, typically less for primary minerals and greater for secondary minerals. These data will be updated once fracture spacings and surface areas are measured or estimated, in addition to having a more detailed geologic model.

Simulated Fluid and Gas Geochemistry and Mineral Alteration

Several types of simulations were performed to evaluate the thermal, hydrological, and chemical factors leading to the observed mineral alteration distribution. These include 2-D simulations using solely the groundwater (WW2) as the initial water composition, and a parallel set of simulations in 1-D to evaluate the effect of different CO_2 and SO_2 fluxes on the fluid geochemistry and mineral alteration distribution as a function of temperature and depth.

Two-dimensional reaction transport simulations were performed assuming an initial unaltered mineral assemblage, steady-state pressures (Figure 5), and the fixed steady-state temperature distribution shown in Figures 6 and 7. Only the primary minerals in Table 3 were present at the initiation of the simulation. For this first set of 2-D simulations it was assumed that there is no flux of magma-derived fluids or gases.

As all the minerals are described by kinetic rates of reaction, the mineral distributions and assemblages change significantly over time. The 2-D simulation discussed in this report was run for 1000 years, but from other 1-D simulations it was found that the mineral proportions change significantly over several thousands of years. However, after 1000 years, the mineral assemblages and their locations tend to stabilize compared to the first few hundred years where minerals disappear and reappear at different depths.

Results show that dissolution of plagioclase, sanidine, cristobalite, and pyroxenes (diopside and hedenbergite) dominate at the depths of the planned EGS reservoir. Plagioclase (albite and anorthite) alteration (as changes from the initial volume %) is particularly intense in the temperature range of 240° to 290°C (Figure 10). Cristobalite is generally unstable in the rhyolitic/tuffaceous rocks and is replaced by the more stable silica polymorph, quartz (Figure 11). Overall, the alteration regions are controlled primarily by temperature, but the extent of dissolution is governed by the lithology.

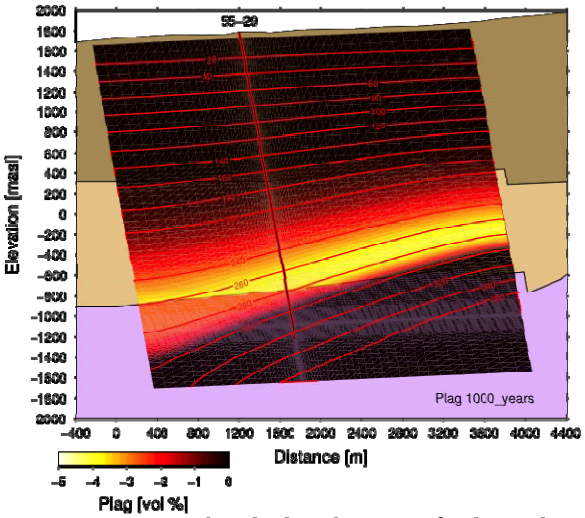

Figure 10: Simulated distribution of plagioclase dissolution (volume %) after 1000 years. Temperature contours are overlain and lithology is shown underlying the model domain.

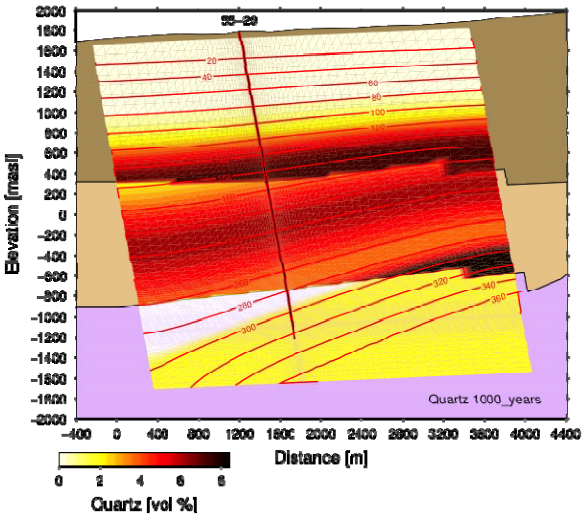

Figure 11: Simulated distribution of quartz precipitation (volume %) after 1000 years.

Within the granodiorite-intruded lavas and tuffs at the depths of the proposed EGS reservoir there is considerable precipitation of quartz, epidote, chlorite (clinochlore and daphnite), and heulandite. In the mud log from NWG 55-29 quartz, epidote, and chlorite are the most commonly observed fracture filling and alteration phases found at depths with measured temperatures over 230°C. Chlorite is a widely seen alteration mineral, and described as interlayered chlorite-smectite at shallower depths, and chlorite at temperatures exceeding about 140°C (Bargar and Keith, 1999). The simulated chlorite distribution is primarily clinochlore and is distributed over nearly the entire domain, with the greatest abundances in the basaltic rocks at the base of the Newberry-Deschutes where temperatures are highest (Figure 12).

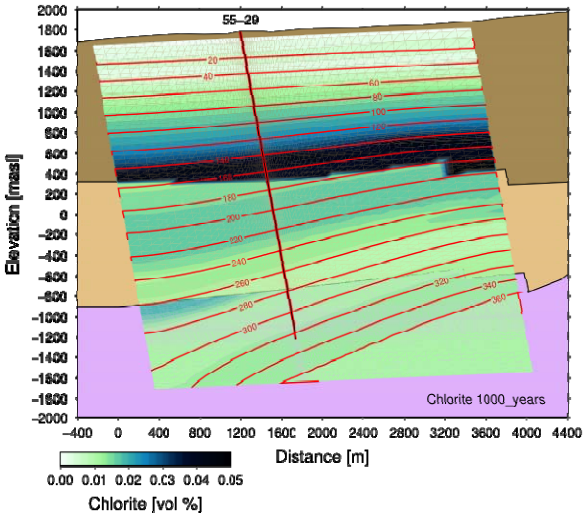

Figure 12: Simulated distribution of chlorite precipitation (volume %) after 1000 years

On the plot of epidote distributions (Figure 13), the observed epidote locations in NWG 55-29 are plotted along the borehole in green. Except for a minor occurrence at a temperature of 207°C, the epidote is distributed from about the 230°C isotherm to the base of the well, as in the simulated distribution. Another band of epidote appearing in the 120°-140°C region in the model, is apparently metastable, since this band was in the process of disappearing by the time the simulation reached 1000 years.

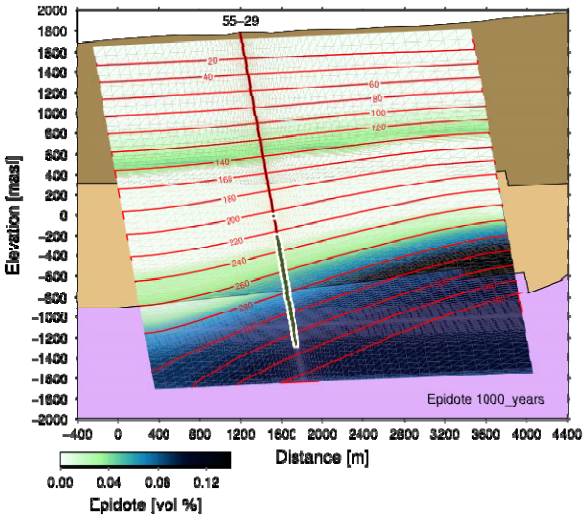

Figure 13: Simulated distribution of epidote precipitation (volume %) after 1000 years. Green shading along drill hole reflects observed epidote in the mud log.

Abundant heulandite is seen in the simulation, where little is observed in the drill hole studies. This discrepancy is likely the result of the low P_{CO2} developed in the system and the destabilization of calcite relative to heulandite. After 1000 years, calcite precipitation is localized in the uppermost kilometer, yet earlier in the simulation had precipitated at much greater depths and temperatures and then redissolved as the P_{CO2} declined.

Whereas the silicate mineral alteration assemblage roughly captures the observed alteration phases at depth (quartz+epidote+chlorite) some inconsistencies in the modeled mineral assemblages include the lack of calcite and pyrite and the addition of substantial heulandite not observed at these depths. The lack of calcite at depth is clearly due to the strong reduction in the partial pressure of CO_2 over time, as there is no external source of CO_2, except from groundwater near the surface. The lack of pyrite is also likely due to the lack of volcanic gas added to the system (i.e., SO_2 and H_2S).

As a simple evaluation of the fluid composition necessary to result in the appearance of calcite and pyrite along with the effects on the entire mineral assemblage, the lower boundary water was modified by successively equilibrating it with CO_2 and SO_2 gas. This boundary fluid then was allowed to interact by aqueous diffusion with a single basal grid block (Intruded John Day) set at 327°C, so that the fluid chemistry could change slowly and the mineral assemblage change owing to the increasing flux of CO_2 (as HCO_3^-) and SO_2 (as a reaction involving SO_4^{-2} and HS^-). In the simulation (Figure 14), pyrite and calcite form after several thousand years, in addition to muscovite, quartz, epidote, clinochlore, daphnite, analcite, and minor hematite.

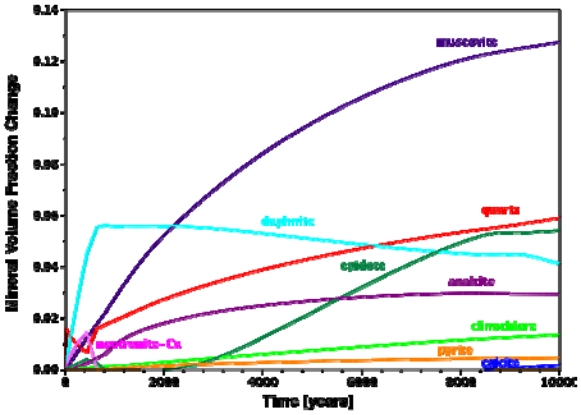

Figure 14: Mineral abundances over time in region having continual addition of magmatic CO_2 and SO_2.

SUMMARY

A native-state and reservoir model of the west flank of Newberry Volcano was created that encompasses the planned stimulation zone and a several km region of the west flank from the surface down to the supercritical region, likely close to a postulated cooling intrusive body. Temperature and pressure distributions were first modeled using TOUGHREACT with boundary conditions estimated from nearby drill holes, and compared to measurements made in the over 3 km deep NWG 55-29 drill hole. With estimates of the porosity and heat capacities for the major hydrogeologic units, thermal conductivities were calibrated by matching to the measured temperature profile. Multicomponent geothermometry was used to estimate potential temperatures of equilibration of waters, and to evaluate the effects of kinetics on calculated mineral equilibration temperatures. To simulate the development of the observed hydrothermal mineralogy, a reaction-transport model (THC) was developed using the pre-alteration mineralogy and shallow groundwater chemistry as the initial geochemical conditions, assuming that modeled temperature and pressure distributions were relatively constant over several thousand years. Close correspondence of modeled and observed epidote distributions support the observation that past hydrothermal activity took place under thermal gradients similar to current values, whereas calcite and sulfide abundances at depth likely require a magmatic gas component. Other than calcite and pyrite, temperature and primary lithology are the overall controls on the alteration mineral distribution.

Current work is now aimed at including mechanical effects of rock deformation and fracture activation during stimulation. New data on fracture distributions, orientations, and stress conditions will be used to further parameterize the multiple continuum model for coupled THMC processes in fractured rock, including estimating the initial permeability distribution, reactive surface areas for fracture coating minerals, and to improve the THMC model. The model now is an effective continuum model, so that the permeability reflects the bulk permeability and the reactivity as well. Since the system is dominantly conductive, with very low permeability, this is a reasonable first approach for the steady-state "native-state" model. Because the mineralogy is primarily a function of temperature, dual permeability would not give different results as a function of depth, but would capture reactivity better. For stimulation, a combined dual-permeability and discrete fracture model in 3-D will be necessary to capture transient thermal and permanent

permeability effects in fractures as done in Sonnenthal et al. (2005).

ACKNOWLEDGEMENTS

This material by supported by the Department of Energy under Award Number DE-EE0002777. Ben Larson (Univ. of Georgia) is acknowledged for assembling some of the preliminary geochemical and groundwater data.

REFERENCES

Bargar, K.E. and Keith, T.E. (1999), "Hydrothermal Mineralogy of Core from Geothermal Drill Holes at Newberry Volcano, Oregon," *U.S. Geological Survey Professional Paper 1578*.

Croucher, A. E. and O'Sullivan, M. J. (2008). "Application of the Computer Code TOUGH2 to the Simulation of Supercritical Conditions In Geothermal Systems," *Geothermics*, **37(6)**, 622-634.

Fitterman, D. V. (1988), "Overview of the Structure and Geothermal Potential of Newberry Volcano, Oregon", *J Geophys Res-Solid*, **93(B9)**, 10059-10066.

Keith, T.E.C. and Bargar, K.E. (1988), "Petrology and Hydrothermal Mineralogy of US Geological Survey Newberry 2 Drill Core From Newberry Caldera, Oregon", *Journal of Geophysical Research*, **93**, 10,174-10,190.

Palandri, J. and Kharaka, Y.K. (2004), "A compilation of rate parameters of water–mineral interaction kinetics for application to geochemical modeling. US Geol. Surv. Open File Report 2004-1068. 64 pp.

Reed M. and Palandri, J., (2006), "SOLTHERM.H06, A Database of Equilibrium Constants For Minerals and Aqueous Species", Available from the authors, University of Oregon, Eugene, Oregon.

Reed M.H. and Spycher N.F. (1984), "Calculation Of pH and Mineral Equilibria in Hydrothermal Waters with Application To Geothermometry and Studies of Boiling and Dilution," *Geochimica et Cosmochimica Acta*, **48**, 1479–1492.

Sammel, E. A., Ingebritsen, S. E., & Mariner, R. H. (1988), "The Hydrothermal System At Newberry Volcano, Oregon," *Journal of Geophysical Research-Solid Earth*, **93(B9)**, 10149-10162.

Sonnenthal, E., Ito, A., Spycher, N., Yui, M., Apps, J., Sugita, Y., Conrad, M. and Kawakami, S. (2005), "Approaches To Modeling Coupled Thermal, Hydrological, and Chemical Processes In The Drift Scale Heater Test At Yucca Mountain," *International Journal of Rock Mechanics and Mining Sciences*, **42**, 698-719.

Spielman, P. and Finger, J. (1998), "Well Test Results Of Exploration Drilling At Newberry Crater, Oregon In 1995", *PROCEEDINGS, Twenty-Third Workshop on Geothermal Reservoir Engineering*, SGP-TR- I58, 22-26.

Xu, T., Spycher, N. F., Sonnenthal, E., Zhang, G., Zheng, L. and Pruess K. (2011), "TOUGHREACT Version 2.0: A Simulator For Subsurface Reactive Transport Under Non-Isothermal Multiphase Flow Conditions," *Computers and Geosciences*, **37**, 763–774.